American Journal of Engineering Research (AJER) 2016
American Journal of Engineering Research (AJER)
e-ISSN: 2320-0847 p-ISSN : 2320-0936
Volume-5, Issue-6, pp-258-265
www.ajer.org
Research Paper Open Access

Flexural Wave Attenuation in A Periodic Laminated Beam

Zhiwei Guo, Meiping Sheng*,Ting Wang
(School Of Marine Science And Technology, Northwestern Polytechnical University, China)

ABSTRACT: *The flexural wave attenuation property of a periodic laminated beam is examined in this paper. The equation of motion of a single laminated beam is firstly derived by Hamilton principle, and then the transfer matrix method and Bloch-Floquet boundary condition are applied to determine the flexural wave band-gaps of an infinite periodic laminated beam. The vibration transmission characteristic is studied by finite element method (FEM), and the numerical result shows that, the band-gaps of an infinite periodic beam from present model match very with the transmittance valleys of a finite periodic beam from FEM model, which shows good accuracy of the present theoretical model. Studies show that, the periodic laminated beam provides good vibration attenuation performance, with broad band-gap widths and strong attenuation ability, thus can be used in the vibration and noise control. The present model derived in this paper can also predict the longitudinal wave propagation property. The Euler model is also examined to give a simple model for convenient purpose in the Engineering applications. The result shows that the simplified model can be used in the low frequency band-gap prediction, while it will induce errors in the high frequency.*

Keywords: *Flexural wave band-gap, Hamilton principle, Transfer matrix method, Periodic laminated beam.*

I. INTRODUCTION

Vibration is a general physical phenomenon when a mechanical structure is excited. Although some vibrations bring beneficial effect, most of the vibration will induce disgusting noise or damage to the mechanical equipment. Thus in order to reduce the vibration, many methods have been proposed. One of them is using periodic structure. Periodic structure consists of periodic identical elements, alternating in the wave propagation direction [1]. It is well known that, the waves in the band-pass propagate while the waves in the band-gap attenuate, because of the Bragg-scattering effect [2] or locally resonant effect [3]. Attracted by the great potential of vibration suppression, extensive studies about periodic structure have been conducted [1, 4, 5].

As beam-type structure is widely used in the engineering applications, the structure periodicity was introduced in the beam-type structure to reduce the vibration in extensive studies. Wen [6] studied the flexural wave propagation of a periodic thin straight beam and discussed the band-gap property caused by Bragg-scattering effect. Yu [7] and Xiao [8] studied the band-gap property of a beam attached with periodic spring-mass systems from numerical simulation and experiment, which gives a physical explanation about the band-gap starting frequency and the cut-off frequency. Wen [9] studied the periodic beam attached with multi-oscillators in order to improve the band-gap performance. Liu [10] studied the periodic curved beam, and obtained some special property compared with the periodic straight beam. There are still a number of works dealing with the periodic beam in various points of view [11-14].

As the composite laminated structure provides high stiffness-to-weight ratio, high strength-to-weight ratio and many other attractive properties [15, 16], it is used widely in the aerospace and ship engineering. However, most of the previous studies about periodic beam are focused on the single layer beam, while the characteristic of periodic laminated beam is not well addressed. In order to solve the vibration control problem met in laminated structure, the wave attenuation property of the periodic laminated beam is studied in this paper. A theoretical model of a multi-layered beam is established in the paper, which will represent the wave propagation and wave attenuation performance. The generally used sandwich structure and the bi-layer structure become the special cases of the current model. The periodic model presented in this paper gives theoretical support of wave attenuation property in the periodic laminated beam and gives a new sight to the vibration control of the composite laminated structure.

II. BAND-GAP FORMULATION BASED ON TIMOSHENKO THEORY

Fig. 1 has shown the model of a periodic laminated beam with *m* layers, alternating with A_i and B_i. Hamilton principle is used to obtain the vibration equations of a single laminated beam.

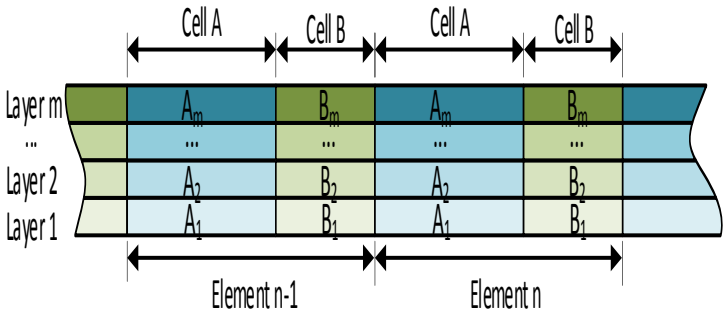

Figure 1: The structure model of a periodic laminated beam.

The single laminated beam is shown in Fig. 2. Assuming that there's no axial slip between two layers, and all the layers have identical transverse displacement w and rotation φ. The shearing deformation and the moment of inertia are considered in the model. The parameters of the i^{th} layer are specified by Young's module E_i, shearing module G_i, density ρ_i, shear coefficient k_i, length L, width b and thickness h_i. Thus, the cross-sectional area is $A_i = bh_i$ and the moment of inertia is $I_i = bh_i^3/12$, respectively. The transverse displacement, longitudinal displacement and the rotation are denoted by w, u_i and φ, respectively.

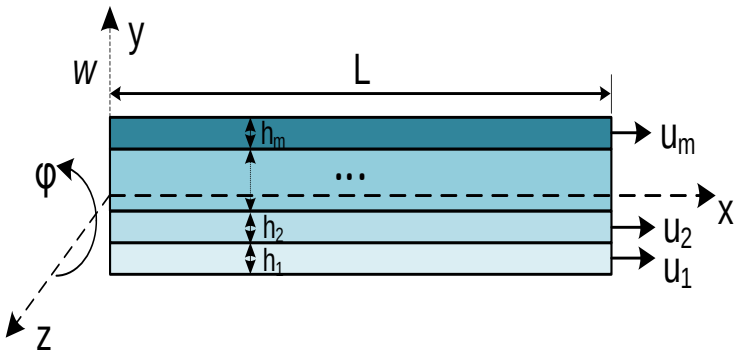

Figure 2: Displacements and dimensions of the single laminated beam.

The longitudinal displacement of the i^{th} layer is,

$$u_i = u_1 + h_{1i}\varphi \tag{1}$$

where $h_{1i} = (h_1 + h_i)/2 + \sum_{j=2}^{i-1} h_j$. The kinematic energy, strain energy and the work done by external forces can be expressed as,

$$E_{kin} = \frac{1}{2}\sum_{i=1}^{m}\int_0^L \left(\rho_i A_i \dot{w}^2 + \rho_i A_i \dot{u}_1^2 + \rho_i I_i \dot{\varphi}^2\right) dx \tag{2}$$

$$E_{pot} = \frac{1}{2}\sum_{i=1}^{m}\int_0^L E_i A_i u_i'^2 + E_i I_i \varphi'^2 + k_i A_i G_i \left(w' - \varphi\right)^2 dx \tag{3}$$

$$W_e = \left(N_1 u_1 + M\varphi + Qw\right)\Big|_0^L \tag{4}$$

Apply Hamilton principle, then the partial differential equations can be obtained as,

$$\begin{cases} \sum_{i=1}^{m} k_i A_i G_i w'' - \sum_{i=1}^{m} \rho_i A_i \ddot{w} - \sum_{i=1}^{m} k_i A_i G_i \varphi' = 0 \\ \sum_{i=1}^{m} E_i A_i u_1'' - \sum_{i=1}^{m} \rho_i A_i \ddot{u}_1 + \sum_{i=2}^{m} h_{1i} E_i A_i \varphi'' - \sum_{i=2}^{m} h_{1i} \rho_i A_i \ddot{\varphi} = 0 \\ \sum_{i=2}^{m} h_{1i} E_i A_i u_1'' - \sum_{i=2}^{m} h_{1i} \rho_i A_i \ddot{u}_1 + \left(\sum_{i=1}^{m} E_i I_i + \sum_{i=2}^{m} h_{1i}^2 E_i A_i \right) \varphi'' \\ \quad - \left(\sum_{i=1}^{m} \rho_i I_i + \sum_{i=2}^{m} h_{1i}^2 \rho_i A_i \right) \ddot{\varphi} - \sum_{i=1}^{m} k_i A_i G_i \varphi + \sum_{i=1}^{m} k_i A_i G_i w' = 0 \end{cases} \tag{5}$$

and the external general forces are,

$$\begin{cases} N_1 = \sum_{i=1}^{m} E_i A_i u_1' + \sum_{i=2}^{m} h_{1i} E_i A_i \varphi' \\ M = \sum_{i=2}^{m} h_{1i} E_i A_i u_1' + \left(\sum_{i=1}^{m} E_i I_i + \sum_{i=2}^{m} h_{1i}^2 E_i A_i \right) \varphi' \\ Q = -\sum_{i=1}^{m} k_i A_i G_i \varphi + \sum_{i=1}^{m} k_i A_i G_i w' \end{cases} \tag{6}$$

As the system is assumed in harmonic oscillation, thus $w(x,t) = W(x)e^{j\omega t}$, $u_1(x,t) = U_1(x)e^{j\omega t}$ and $\varphi(x,t) = \Phi(x)e^{j\omega t}$. Substituting these expression into (5) gives,

$$W^{(6)} + c_1 W^{(4)} + c_2 W^{(2)} + c_3 W = 0 \tag{7}$$

$$\begin{cases} U_1' = d_1 W^{(4)} + d_2 W^{(2)} + d_3 W \\ \Phi' = e_1 W^{(2)} + e_2 W \end{cases} \tag{8}$$

The solution of (7) can be assumed as $W(x) = W_0 e^{\lambda x}$. Substituting this expression into (7) gives the following polynomial equation,

$$\lambda^6 + c_1 \lambda^4 + c_2 \lambda^2 + c_3 = 0 \tag{9}$$

Six roots can be obtained as λ_1、λ_2、λ_3、λ_4、λ_5 and λ_6 by solving (9). Taking account of (5-9) gives,

$$\begin{cases} W = \sum_{j=1}^{6} T_j e^{\lambda_j x}; \quad U_1 = \sum_{j=1}^{6} \alpha_j T_j e^{\lambda_j x}; \quad \Phi = \sum_{j=1}^{6} \beta_j T_j e^{\lambda_j x} \\ N_1 = \sum_{j=1}^{6} b_{1j} T_j e^{\lambda_j x}; \quad M = \sum_{j=1}^{6} b_{2j} T_j e^{\lambda_j x}; \quad Q = \sum_{j=1}^{6} b_{3j} T_j e^{\lambda_j x} \end{cases} \tag{10}$$

If we make $\boldsymbol{\psi} = [T_1 \quad T_2 \quad T_3 \quad T_4 \quad T_5 \quad T_6]^{\mathrm{T}}$, $\boldsymbol{D}_0 = [U_{1,0} \quad \Phi_0 \quad W_0 \quad N_{1,0} \quad M_0 \quad Q_0]^{\mathrm{T}}$ and $\boldsymbol{D}_L = [U_{1,L} \quad \Phi_L \quad W_L \quad N_{1,L} \quad M_L \quad Q_L]^{\mathrm{T}}$, we can obtain that,

$$\begin{cases} \boldsymbol{D}_0 = \boldsymbol{B}\boldsymbol{\psi} \\ \boldsymbol{D}_L = \boldsymbol{C}\boldsymbol{\psi} \end{cases} \tag{11}$$

where $\boldsymbol{B}$ and $\boldsymbol{C}$ are 6×6 matrixes, and $\boldsymbol{D}_0$ and $\boldsymbol{D}_L$ are the state vectors at $x = 0$ and $x = L$.

The transfer matrix method is used to calculate the band-gap frequency. As shown in Fig. 3, the unit element is constituted by cell A and cell B, with length L_A and L_B. By using (11), the state vectors of cell A can be expressed as $\boldsymbol{D}_{10} = \boldsymbol{B}_1\boldsymbol{\psi}_1$ and $\boldsymbol{D}_{1L} = \boldsymbol{C}_1\boldsymbol{\psi}_1$, and those of cell B can be expressed as $\boldsymbol{D}_{20} = \boldsymbol{B}_2\boldsymbol{\psi}_2$ and $\boldsymbol{D}_{2L} = \boldsymbol{C}_2\boldsymbol{\psi}_2$, respectively.

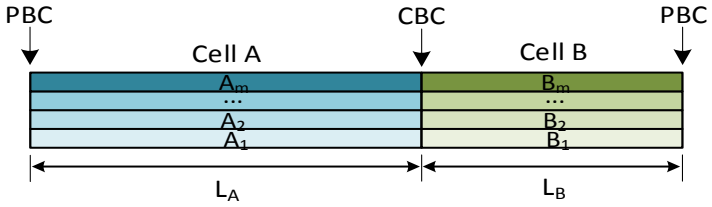

Figure 3: The components of a unit element and the boundary conditions.

The continuous boundary condition (CBC) at the interface between cell A and cell B can be expressed as,

$$\boldsymbol{D}_{1L} = \boldsymbol{D}_{20} \tag{12}$$

and the periodic boundary condition (PBC) between cell A and cell B can be expressed as,

$$\boldsymbol{D}_{10} = e^{-iqL}\boldsymbol{D}_{2L} \tag{13}$$

where q is the wavenumber along the axil direction, with real part representing the wave propagation property, and the imaginary part representing the wave attenuation property. The lattice constant is $L = L_A + L_B$.

Taking account of (12, 13) gives,

$$\left(\boldsymbol{T} - e^{iqL}\boldsymbol{I}\right)\boldsymbol{\psi}_1 = 0 \tag{14}$$

where $\boldsymbol{I}$ is the identity matrix and $\boldsymbol{T} = \boldsymbol{B}_1^{-1}\boldsymbol{C}_2\boldsymbol{B}_2^{-1}\boldsymbol{C}_1$.

For a given frequency f_0, we can obtain from (14) that,

$$\left|\boldsymbol{T}(f_0) - e^{iqL}\boldsymbol{I}\right| = 0 \tag{15}$$

The wavenumber q can be obtained by solving the above equation. And then the dispersion curves (frequency vs wavenumber) can be obtained and the band-gap property is then determined. The band-gaps of both flexural wave and longitudinal wave can be acquired by (15). As the emphases of this paper is on the flexural wave, the following text will focus on the flexural wave band-gap property.

III. NUMERICAL EXAMPLE

A sandwich beam is considered in this numerical example, as it is most widely used among the laminated structures. Thus each element is constituted by six components, including A_1, A_2, A_3, B_1, B_2 and B_3. The material properties of each component are shown in Table 1. The lengths and widths of cell A and cell B are set as L_A=0.15m, L_B=0.1m and b_A=b_B=0.015m. From bottom to top, the thicknesses are set as h_1=0.003m, h_2=0.002m and h_3=0.002m.

The flexural wave band-gaps are shown in Fig. 4. In the figure, three band-gaps exist below 2000 Hz, and the band-gaps are 55.7~96.0 Hz, 266.3~837.1 Hz and 1059.3~1525.3 Hz, with the band-gap widths of 40.3 Hz, 570.8 Hz and 466.0 Hz, respectively. This periodic laminated beam performs very well in the band-gap property with the total band-gap of 1077.1 Hz, which indicates that, more than half of the wave below 2000 Hz are suppressed. The imaginary part of the wavenumber is called decay constant, as it represents the attenuation ability of the periodic laminated beam. As shown in Fig. 4(b), the decay constant of the first band-gap is 0.11, which is smaller than 0.57 in the second band-gap and 0.37 in the third band-gap. Resulting that the decay ability of the first band-gap is weaker than the second and the third band-gap. Also the first band-gap bandwidth is very narrow, thus the attenuation performance of the first band-gap is inferior to the second and the third band-gaps. Therefore, the second band-gap is most important in the engineering application in general vibration control, because of its low frequency, strong attenuation ability and broad band-gap bandwidth. However, for the low-frequency line spectrum vibration control, the first band-gap can also have good performance, as the target frequency of vibration control is very narrow.

Table 1: Material properties of each component in an element.

Material property	A_1	A_2	A_3	B_1	B_2	B_3
Young's module (GPa)	210.6	77.6	210.6	2	4.35	2
Shear module (GPa)	81	28.7	81	0.72	1.59	0.72
density (kg/m^3)	7780	2730	7780	1142	1180	1142
Shear coefficient	5/6	5/6	5/6	5/6	5/6	5/6

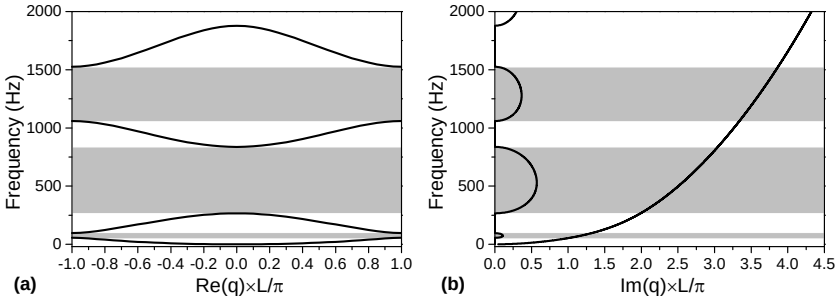

Figure 4: The band gaps of flexural vibration with (a) the real part of normalized wavenumber and (b) the imaginary part of normalized wavenumber.

The present model is validated by the FEM analysis with an eight-element finite periodic laminated beam, which is shown in Fig. 5. The material and geometry parameters for a unit element are the same as the parameters in the above theoretical model. The unit harmonic displacement excitation is applied at the left beam end, and the displacement response is measured at the right beam end. The vibration response are shown in Fig. 6, where the shaded region are the band-gaps calculated from the theoretical model. As shown in the figure, the response valleys of the finite periodic beam in the FEM model match very well with the band-gaps of the infinite periodic beam in the theoretical model. Thus the present model has a good performance in the band-gap predictions.

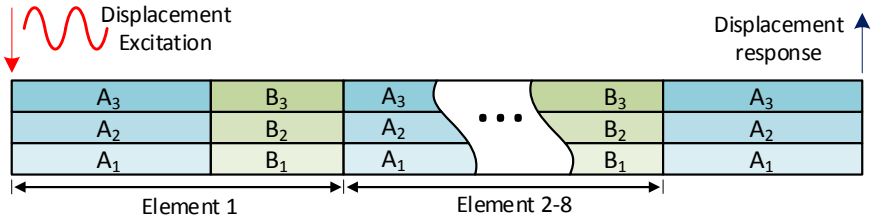

Figure 5: The FEM model of a periodic laminated beam.

As shown in Fig. 6, the periodic laminated beam behaves as a wave filter, with the waves in the band-passes propagating freely without attenuation and the waves in the band-gaps being attenuated. Thus the present periodic laminated beam can be used in the vibration control by designing the band-gaps at the frequency range where the vibration need to be controlled. For an eight-element periodic beam, the average attenuation levels in the first three band-gaps reach respectively to 19.3 dB, 74.3 dB and 30.9 dB, which shows good attenuation performance and are very attractive in the vibration control.

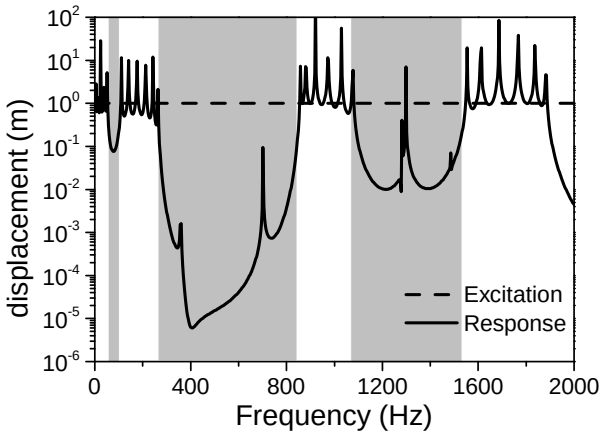

Figure 6: The flexural vibration transmission characteristic of a finite periodic sandwich beam. (The shadow region are the band gaps obtained from theoretical model.)

IV. SIMPLIFIED MODEL

In the Timoshenko model, the shearing deformation and the moment of inertia are considered, resulting a very complicated model, which will induce an ill-conditioned matrix in some frequencies. Thus high resolution numerical methods are needed to solve the above problem. In order to make it convenient in the engineering application, the simplified Euler mode is also studied to obtain the band-gap property. And a simple principle about which model should be used at specific situation is given as a guideline in this section.

Each layer is considered as an Euler-beam, and the multi-layer beam is modeled as an equivalent single layer beam by calculating the equivalent bending rigidity and the equivalent density. The spatial force analysis is shown in Fig. 7.

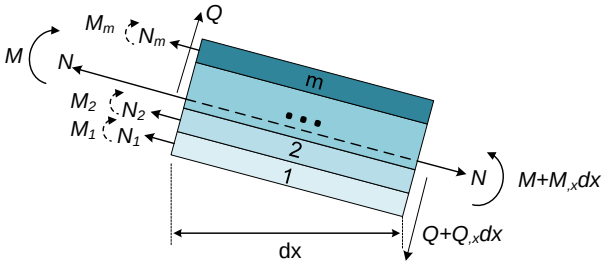

Figure 7: The spatial forces analysis sketch of a laminated beam.

From (1), we can obtain that $u_i = u_1 + w' h_{1i}$ $(i = 2 \sim m)$, where w' is the derivation of transverse displacement w with respect to x, and h_{1i} is the distance between the midline of the 1st layer and the i^{th} layer. From the relation of longitudinal displacement and the strain $\varepsilon_i = u_i'$, we can obtain $\varepsilon_i = \varepsilon_1 + w'' h_{1i}$. Thus the axial force of each layer can be expressed as,

$$N_i = E_i A_i \left(\varepsilon_1 + w'' h_{1i} \right) \tag{16}$$

and the axial forces are balanced by $\sum_{i=1}^{m} N_i = 0$. Substituting (16) into the summation gives,

$$\sum_{i=1}^{m} E_i A_i \left(\varepsilon_1 + w'' h_{1i} \right) = 0 \tag{17}$$

From (17), we can obtain,

$$\varepsilon_1 = \alpha w'' \tag{18}$$

where $\alpha = -\sum_{i=1}^{m} E_i A_i h_{1i} \Big/ \sum_{i=1}^{m} E_i A_i$. The total moment of the laminated beam can be expressed as,

$$M = \sum_{i=1}^{m} M_i - \sum_{i=1}^{m} N_i h_{1i} \tag{19}$$

where $M_i = -E_i I_i w''$. Substituting M_i and (16) into (19) gives,

$$M = -\overline{EI} w'' \tag{20}$$

where $\overline{EI} = \sum_{i=1}^{m} E_i I_i + \sum_{i=1}^{m} E_i A_i \left(\alpha + h_{1i} \right) h_{1i}$. Thus the equivalent bending rigidity $\overline{EI}$ is determined. As the equivalent density can be calculated as $\overline{\rho} = \sum_{i=1}^{m} \rho_i A_i \Big/ \sum_{i=1}^{m} A_i$. Therefore, the equivalent equation of motion for a laminated beam can be expressed as,

$$\overline{EI} \frac{\partial^4 w}{\partial x^4} = -\overline{\rho} A \frac{\partial^2 w}{\partial t^2} \tag{21}$$

According to the plane wave extension method of a single layer beam [6], the band-gap frequency can finally be determined.

V. PERFORMANCE COMPARISON

The flexural wave dispersion curves and the band-gaps of the Timoshenko model and the Euler model are compared in Fig. 8 and Table 2. As shearing deformation and moment of inertial are ignored, the Euler model will bring some errors. As shown in Fig. 8, the first four dispersion curves of the Euler model nearly coincidence with those of the Timoshenko model. Thus the Euler model has high accuracy in the first four dispersion curves. From the fifth dispersion curve, with the increase curve order, the error of the Euler model increases. The frequency difference of the two models reaches as much as about 1000 Hz for the eighth dispersion curve. The band-gap frequencies and the band-gap widths for the two models are shown in Table 2. We can see that, with the increase of band-gap order, the error increases gradually. From the first to the seventh band-gap, the band-gap starting frequency error increases from 0.1 Hz to 509.8 Hz, and the relative error increases from 0.2% to 9.2%; the band-gap cut-off frequency error increases from 0.7 Hz to 1007.9 Hz, and the relative error increases from 0.7% to 14.4%.

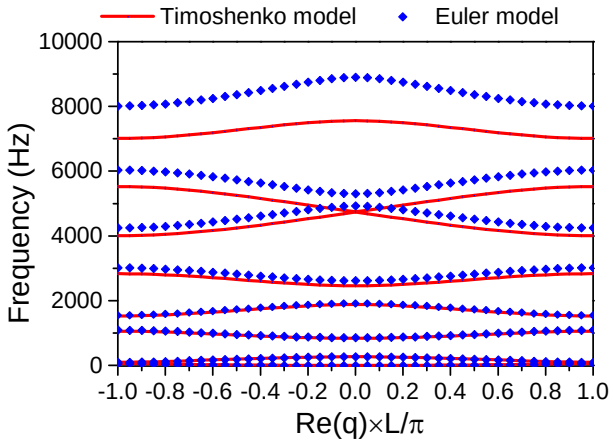

Figure 8: The dispersion curves comparison between two models.

Table 2: The band-gap frequency comparison between two models.

Band-gap order	Starting frequency/Hz		Error /Hz	Relative Error	Cut-off frequency/Hz		Error /Hz	Relative Error
	Timoshenko	Euler			Timoshenko	Euler		
1	55.7	55.8	0.1	0.2%	96.0	96.7	0.7	0.7%
2	266.3	268.5	2.2	0.8%	837.1	857.7	20.6	2.5%
3	1059.3	1093.1	33.8	3.2%	1525.3	1550	24.7	1.6%
4	1878.3	1912.1	33.8	1.8%	2460.3	2623.1	162.8	6.6%
5	2831.6	3018.5	186.9	6.6%	4003.7	4249.3	245.6	6.1%
6	4734.1	4927.3	193.2	4.1%	4743.0	5307.7	564.7	11.9%
7	5525.3	6035.1	509.8	9.2%	7010.5	8018.4	1007.9	14.4%

Thus we can see, the simplified model gives accurate results for the low frequency flexural wave band-gaps, and will bring significant error when it comes to high frequency wave band-gaps. That's because a low frequency is associated with a big wave length, and the effects caused by the shearing deformation and moment of inertia are relatively small, which can be ignored, thus the Euler model gives an accurate result. While for the high frequency wave, the wave length is short, and the shearing deformation and moment of inertia have significant effects on the mode frequencies and then on the band-gaps. Ignoring these effects gives rise to significant error. When the effects of shearing deformation and moment of inertia are not considered, the equivalent bending rigidity is enhanced, resulting that the dispersion curve frequencies are overestimated in the Euler model, which can be checked in Fig. 8 and Table 2.

Therefore, in the engineering application of a periodic laminated beam, when the low frequency band-gaps are calculated, the Euler model can be used because of its simplicity and satisfactory result. However, when the high frequency band-gaps are calculated, the Timoshenko model must be used as it gives more accurate result.

VI. CONCLUSIONS

The band-gap characteristic of the periodic laminated beam is examined with Hamilton principle and transfer matrix method. The present theoretical model shows high accuracy and is validated by FEM. For the flexural wave, this periodic structure owns excellent band-gap attenuation performance below 2000 Hz, with more than half of the waves in frequency domain are attenuated. The first and second band-gap locate at low

frequency region, thus the periodic laminated beam gives a new method to solve the low frequency vibration control problem. Although the first band-gap is narrow, it still has potentials in the line spectral vibration control. The present model derived in this paper can also give the longitudinal wave propagation property, which lays the foundation to the future study about the coupled wave propagation property between the flexural and longitudinal waves. The simplified Euler model gives accurate result for the first several dispersion curves, thus can predict low frequency band-gaps in the engineering application. In the high frequency, the Euler model will bring significant error, and the Timoshenko model must be applied.

REFERENCES

[1]. D. M. Mead, Wave propagation in continuous periodic structures: Research contributions from southampton, 1964–1995, Journal of Sound and Vibration, 190(3), 1996, 495-524.

[2]. D. Sutter-Widmer, S. Deloudi and W. Steurer, Prediction of bragg-scattering-induced band gaps in phononic quasicrystals, Physical Review B, 75(9), 2007, 094304.

[3]. Z. Liu, X. Zhang, Y. Mao, Y. Y. Zhu, Z. Yang, C. T. Chan and P. Sheng, Locally resonant sonic materials, Science, 289(5485), 2000, 1734-1736.

[4]. M. I. Hussein, M. J. Leamy and M. Ruzzene, Dynamics of phononic materials and structures: Historical origins, recent progress, and future outlook, Applied Mechanics Reviews, 66(4), 2014, 040802.

[5]. D. Del Vescovo and I. Giorgio, Dynamic problems for metamaterials: Review of existing models and ideas for further research, International Journal of Engineering Science, 80, 2014, 153-172.

[6]. J. Wen, D. Yu, G. Wang, H. Zhao, Y. Liu, X. Dang, Y. Tan, K. Zuo, L. Chen and Y. Zhang, Elastic wave band gaps in flexural vibrations of straight beams, Chinese Journal of Mechanical Engineering, 41(4), 2005, 1-6.

[7]. D. Yu, Y. Liu, G. Wang, H. Zhao and J. Qiu, Flexural vibration band gaps in timoshenko beams with locally resonant structures, Journal of Applied Physics, 100(12), 2006, 124901.

[8]. Y. Xiao, J. Wen, D. Yu and X. Wen, Flexural wave propagation in beams with periodically attached vibration absorbers: Band-gap behavior and band formation mechanisms, Journal of Sound and Vibration, 332(4), 2013, 867-893.

[9]. Y. Xiao, J. Wen and X. Wen, Flexural wave band gaps in locally resonant thin plates with periodically attached spring–mass resonators, Journal of Physics D: Applied Physics, 45(19), 2012, 195401.

[10]. S. Liu, S. Li, H. Shu, W. Wang, D. Shi, L. Dong, H. Lin and W. Liu, Research on the elastic wave band gaps of curved beam of phononic crystals, Physica B: Condensed Matter, 457, 2015, 82-91.

[11]. D. J. Mead and Š. Markuš, Coupled flexural-longitudinal wave motion in a periodic beam, Journal of Sound and Vibration, 90(1), 1983, 1-24.

[12]. G. Wang, J. Wen and X. Wen, Quasi-one-dimensional phononic crystals studied using the improved lumped-mass method: Application to locally resonant beams with flexural wave band gap, Physical Review B, 71(10), 2005, 104302.

[13]. P. Cartraud and T. Messager, Computational homogenization of periodic beam-like structures, International Journal of Solids and Structures, 43(3), 2006, 686-696.

[14]. R. Zhu, X. N. Liu, G. K. Hu, C. T. Sun and G. L. Huang, A chiral elastic metamaterial beam for broadband vibration suppression, Journal of Sound and Vibration, 333(10), 2014, 2759-2773.

[15]. A. P. Mouritz, E. Gellert, P. Burchill and K. Challis, Review of advanced composite structures for naval ships and submarines, Composite Structures, 53(1), 2001, 21-42.

[16]. R. F. Gibson, A review of recent research on mechanics of multifunctional composite materials and structures, Composite Structures, 92(12), 2010, 2793-2810.